

Optimal Titan Trajectory Design Using Invariant Manifolds and Resonant Gravity Assists

Final Summer Undergraduate Research Fellowship Report

September 25, 2009

Natasha Bosanac

Mentor: Professor Jerrold E Marsden, Ashley Moore, Stefano Campagnola

Abstract

Through a combination of invariant manifolds in the planar circular restricted three body problem and multiple resonant gravity assists, it is possible to design trajectories with a ΔV significantly smaller than that for a typical Hohmann transfer. In this paper, the Keplerian mapping function will be explored as a means to choose desirable resonances rather than taking advantage of the maximum available energy kick. The goal is to create a resonant gravity assist trajectory which will, at any single node, minimize time of flight and exposure to significant perturbations. Using this design tool, the resulting time of flight for a trajectory at a single Jacobi constant will be compared with a trajectory utilizing the maximum decrease in semimajor axis at any single point. Through selecting desired resonances, the effect of the Jacobi constant on the trajectory's total ΔV is explored.

1. Introduction

In recent years, Cassini's primary mission has delivered a wealth of knowledge about Saturn's largest, haze-covered moon, Titan. Amongst other outcomes of the mission, Cassini has revealed that the surface of Titan features equatorial sand dunes and liquid oceans – resembling the early state of the Earth billions of years ago. Given this analogous behavior, NASA maintains plans for a future collaboration with ESA to explore the surface of Titan with a lighter-than-air vehicle.

One constraint imposed on such a mission is the limitation on fuel in navigating a distance as far as Saturn and its moons. Careful trajectory design can decrease the spacecraft's fuel requirement, thereby easing the constraints on other subsystems and allowing additional mission objectives.

The Keplerian mapping function is explored as a means to choose desirable resonances rather than taking advantage of the maximum available energy kick. Resonant gravity assist trajectories are created such that at any single node, a decision is made to minimize time of flight and exposure to significant perturbations. Using this design tool, a large decrease in time of flight is found when compared with a trajectory utilizing the maximum decrease in semimajor axis at any single point. Next, the effect of the Jacobi constant on the trajectory's total ΔV is explored. The particular choice of Jacobi constant is shown to affect the position of the invariant manifold Poincarè section taken at periapsis when plotted in Keplerian mapping space and the sequence of resonances that can be traversed to target this exit region.

2. Targeting Better Resonances

Construction of the gravity assist portion of the trajectory relies on the following problem definition: two main bodies, referred to as primaries, revolve around their barycenter with a test mass, the spacecraft, moving in a near Keplerian orbit under the influence of the gravitational attraction of the primaries. The spacecraft begins in an orbit of large semimajor axis about Saturn. By iteratively employing resonant gravity assists, it is possible to decrease the semimajor axis of the spacecraft orbit such that it can target the invariant manifolds in the Saturn-Titan system.¹ The largest perturbation occurs at the periapsis of the spacecraft's orbit, which can be described by two key parameters: the argument of periapsis, ω , and the Keplerian energy, $K = \frac{-1}{2a}$. This change in semimajor axis can be modeled as an instantaneous kick approximated by an energy kick function, f . Considering the effect of the gravitational force on the semi-major axis, and therefore the Keplerian energy, the following two-dimensional map² can approximate

the sequence of periapsis coordinates (ω_n, K_n) , $n=1, 2, 3, \dots$, from an initial (ω_0, K_0) with the application of control u_n :

$$F \begin{pmatrix} \omega_n \\ K_n \end{pmatrix} = \begin{pmatrix} \omega_{n+1} \\ K_{n+1} \end{pmatrix} = \begin{pmatrix} \omega_n - 2\pi(-2K_{n+1})^{-\frac{3}{2}} \pmod{2\pi} \\ K_n + \mu f(\omega_n) + \alpha u_n \end{pmatrix} \quad (1)$$

$$\text{Where } \alpha = \sqrt{\frac{1}{\bar{a}} \left(\frac{1+\bar{e}}{1-\bar{e}} \right)} \text{ with } \bar{e} = \sqrt{1 - \left(\frac{C_J - \bar{a}}{2\bar{a}^{3/2}} \right)^2} \text{ and } \bar{a} = -\frac{1}{2K} \quad (2)$$

One can also define the Jacobi constant as a measure of the energy of the spacecraft. If:

$$E(x, y, \dot{x}, \dot{y}) = \frac{1}{2}(\dot{x}^2 + \dot{y}^2) - \Omega(x, y) \quad (3)$$

where

$$\Omega(x, y) = \frac{x^2 + y^2}{2} + \frac{1 - \mu}{\sqrt{(x + \mu)^2 + y^2}} + \frac{\mu}{\sqrt{(x - 1 + \mu)^2 + y^2}} \quad (4)$$

then the Jacobi constant is then $C_J = -2E$.³

Any resonance can be described as a ratio, $n:m$, where n is the number of Titan revolutions about Saturn and m is the number of spacecraft revolutions about Saturn.⁴ The term ‘better resonance’ describes a resonance where n is as low as possible. Since n is proportional to the period of Titan’s orbit about Saturn, this means a decrease in the time of flight for the spacecraft. In addition, the larger the difference in $n-m$, the more susceptible the spacecraft orbit is to extra perturbation as it passes through the region of maximum energy kick $n-m$ times.

An example plot of the achievable change in semimajor axis starting from $a=1.48$ for a Jacobi constant of $C_J = 3.012$ is shown in Figure 1. Given an initial semimajor axis, a_n , the dotted blue line indicates the next semimajor axis, a_{n+1} , if the spacecraft has an initial argument of periapsis, w_n , for 0 m/s of ΔV . Similarly, the solid blue line indicates the successive semimajor axis for 10 m/s of ΔV applied at the initial periapsis. The colored lines represent resonances which are labeled on the right hand side: thicker lines have a larger $n-m$ value (where n is the number of Titan revolutions and m refers to spacecraft revolutions) while lines that are closer to the red side of the ROYGBIV color scale have a lower n value.

Figure 1a) suggests that for a given control input, the succeeding resonance, $(n:m)_{n+1}$, can be chosen and reached by using ΔV ’s during the initial resonance, $(n:m)_n$, to target ω_n . It also suggests that by increasing the ΔV used at the initial periapsis, (ω_n, K_n) , one could increase the range of available resonances to consider when designing a low energy trajectory. Expanding on

this idea, Figure b), which is a subset region of a), features two red dots at the maximum semimajor axis, a_{n+1} , achievable for a given initial semimajor axis. As expected from the Keplerian map approximation (Equation 1), a ΔV of 10 m/s yields a larger semimajor axis change than the uncontrolled iterate. However, simply exploiting the largest possible change in semimajor axis will lead the spacecraft to resonances such as the 18:11 and 13:8 resonances. Instead of jumping to these resonances which take a long time to travel through, one could jump to the 5:3 resonance by targeting the range of initial periapsis angles indicated by the red box. Although it may not yield the largest possible decrease in semimajor axis, it does decrease the time required to complete this portion of the trajectory.

Through a combination of invariant manifolds of the planar circular restricted three body problem and multiple resonant gravity assists, it is possible to design trajectories to Titan with a ΔV significantly smaller than that for a typical Hohmann transfer.¹ Employing the aforementioned method of targeting desired resonances, one can successively use resonant gravity assists to decrease the semimajor axis of the spacecraft orbit until it gets close to the region of (ω_n, K_n) coordinates that correspond to the invariant manifolds. As shown by the red curve in Figure 2, this exit region corresponds to a Poincarè section taken at periapsis for the trajectories comprising the Saturn-Titan stable manifolds. While a trajectory can be designed to target this exit region, the assumption of a near-Keplerian orbit breaks down close to the secondary body, Titan.⁵

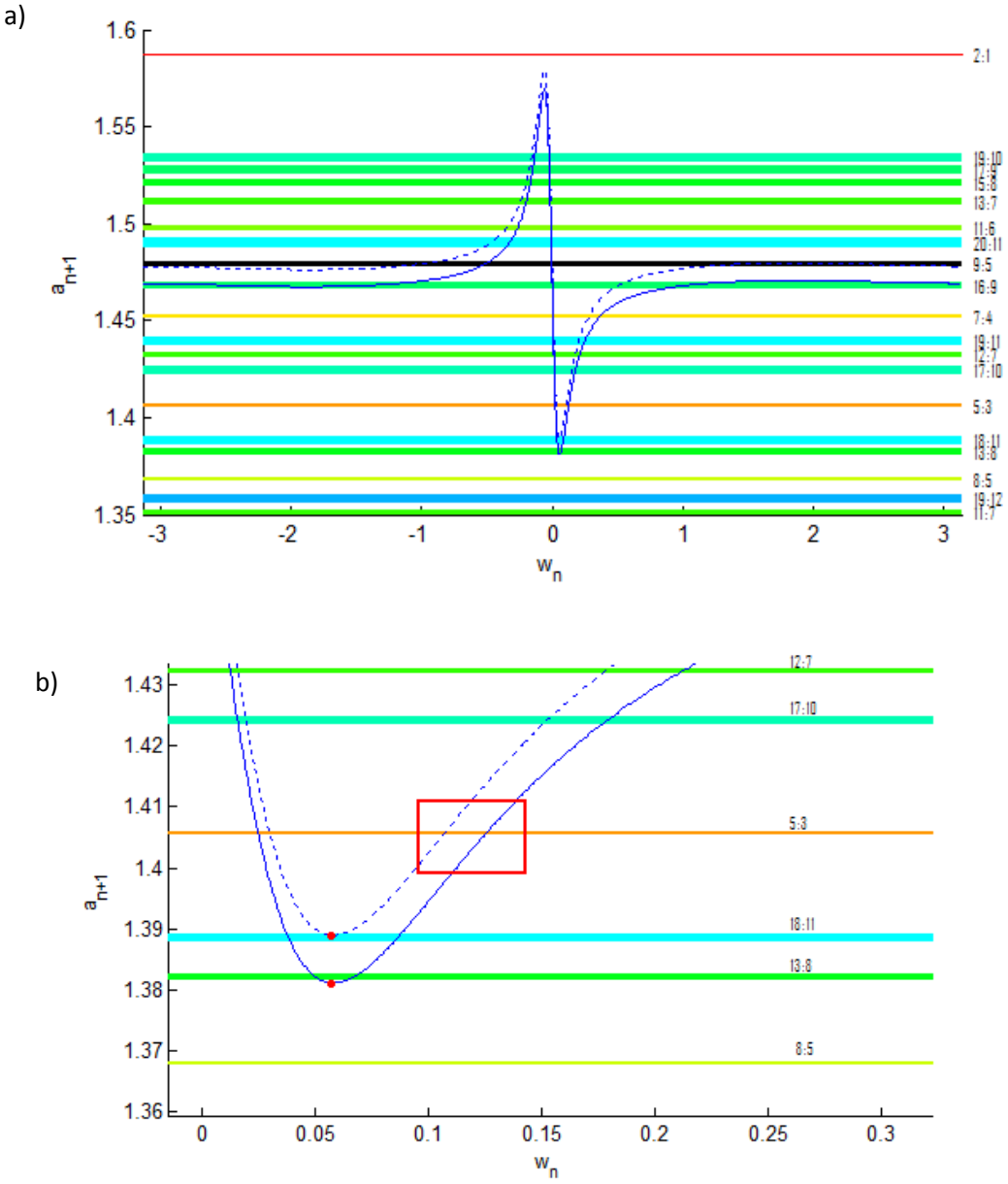


Figure 1: Starting from an initial semimajor axis, a_n , of 1.48, a) shows the reachable semimajor axis a_{n+1} for varying values of initial periapsis angle, ω_n . The dotted blue line evaluates the energy kick for 0 m/s of ΔV while the solid blue line uses a maximum 10 m/s of ΔV applied at periapsis. A subset of this is shown in b) to demonstrate the resonances that will be reached using the maximum energy kick. The red box indicates that a better resonance can still yield a large decrease in semimajor axis.

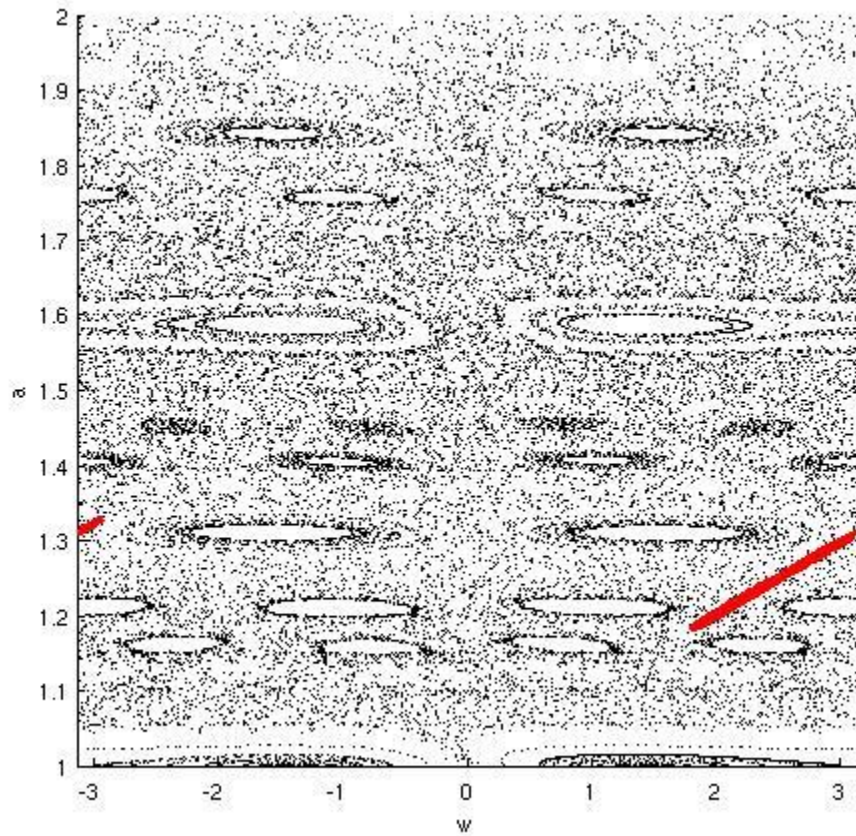


Figure 2 : Keplerian map for the Saturn-Titan system, assuming $C_J = 3.012$ and an average semimajor axis of 1.55. The white holes indicate stable resonant islands, while the red curve represents the target region corresponding to the Poincaré section of the stable manifold at periapsis.

In order to demonstrate the benefit of selecting the sequence of resonances rather than exploiting an instantaneous maximum decrease in semimajor axis, two trajectories have been created for an example Jacobi constant, $C_J = 3.012$. A trajectory utilizing the absolute maximum energy kick available to move between resonances is shown in Figure 3 - using merely 30.9 m/s, which is an extremely small value of ΔV for such a far journey. While this procedure may utilize the maximum available decrease in semi-major axis over each jump between resonances, it does not target good resonances. In fact, the spacecraft travels along the sequence 24:11 – 2:1 – 19:10 – 30:17 – 11:7, meaning that the trajectory has a time of flight approximately equal to 86 Titan revolutions.

One can compromise when selecting a desired sequence of resonances by performing a trade-off between fewer Titan revolutions (lower n value) and a significant decrease in

semimajor axis. This has been implemented by considering only the resonances available for an initial periapsis angle on the interval $\omega = (0, 0.15]$. Although the exact upper limit of this interval is not a fixed boundary, it does provide the benefits of simultaneously allowing a wide range of resonances and significantly decreasing the semimajor axis. Since this resonance may be reached with a finite interval of values for control input, the author finds the desired periapsis angle for the lowest required amount of control input – subtly enforcing the objective of using the least fuel possible. Employing this technique has created the trajectory shown in Figure 4 which requires a ΔV of 15.99 m/s over the entire resonant gravity assist portion of the trajectory and travels along the sequence of resonances 11:5 - 2:1 - 9:5 - 5:3 - 3:2 - 7:5. Thus, this part of the trajectory has a time of flight approximately equal to 37 Titan revolutions.

It thus becomes clear that traveling along carefully selected resonances is a subtle form of decreasing the trajectory time of flight. If one were to simply input an initial trajectory such as that in Figure 3 into an optimization algorithm and consider time of flight in the cost function, it would only minimize the travel time for a given sequence of resonances. Instead, better resonances can be reached by targeting specific periapsis angles which do not necessarily correspond to those that result in the maximum decrease in semimajor axis. In addition, it allows for a decrease in the sum of $n-m$ for each of the resonances, and thus decreases the extra perturbations as it passes through the region of high energy kick $n-m$ times. This implies that a good resonant gravity assist trajectory will be created by considering the maximum change in semimajor axis per Titan revolution rather than simply the maximum total change in semimajor axis between two resonances.

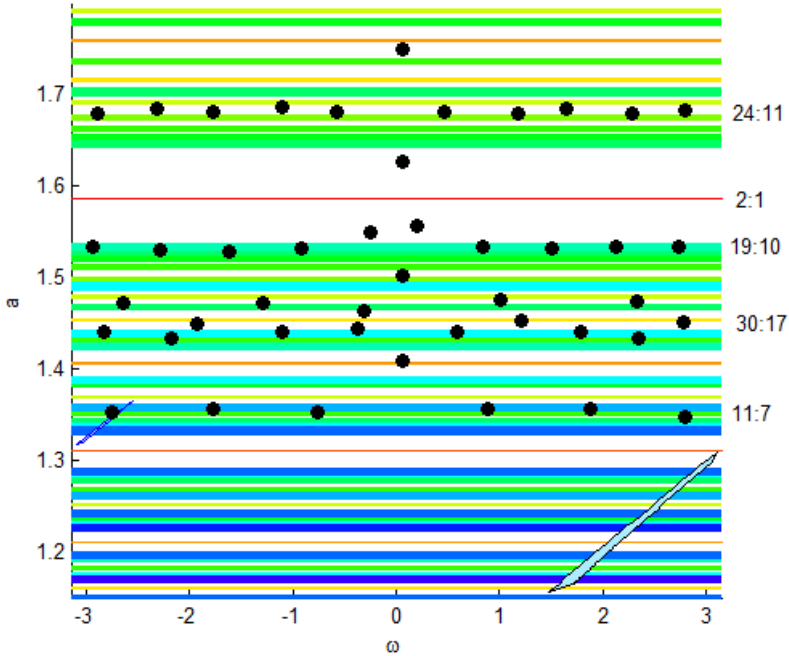


Figure 3 : Resonant gravity assist trajectory plotted as blue points on top of the Keplerian map. Note the final node in (ω, K) space that intersects the red curve representing the stable manifold on the bottom left of the figure. This portion of the trajectory uses a ΔV of only 30.8 m/s.

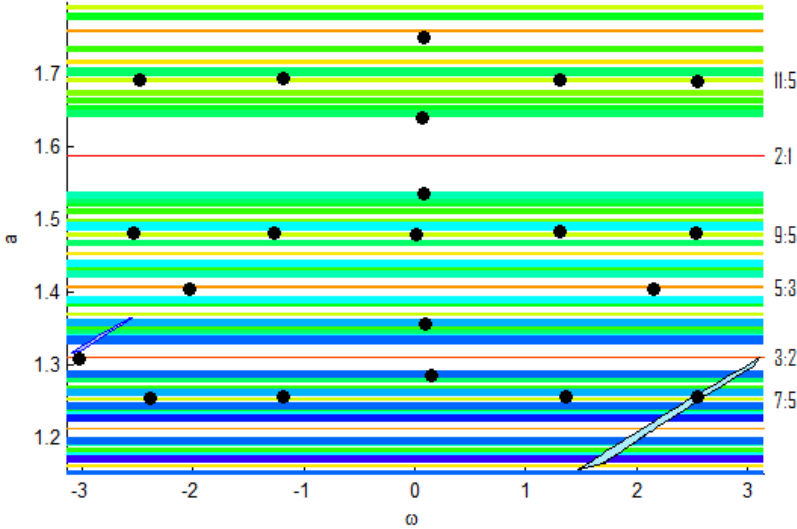


Figure 4: Resonant gravity assist produced with selective resonance targeting for $C_J=3.012$ plotted as black points and target regions shown in light blue in the bottom of the figure. These points of interest are plotted against resonances, with those traversed labeled on the right.

3. Varying the Jacobi Constant

In order to travel from the exterior Hill’s region to the interior region, the Jacobi constant of the spacecraft must remain within the range $E(L_2) < E < E(L_3)$.³ For the Saturn-Titan system, this interval becomes $3.0157 < E < 3.005$. Varying the Jacobi constant within this range will change the Poincarè section of the stable invariant manifold, thereby changing the region that the resonant gravity assist portion of the trajectory must target. In addition, the sequence of resonances is also affected, as well as the set of resonances that both intersect the exit region and allow a periapsis coordinate to fall within the region given a maximum value of control input. The exact interaction of these effects poses an interesting problem with respect to mission design.

Such a study was implemented by carrying out the steps detailed in Section 2: generate the invariant manifolds, take a Poincarè section at periapsis for the stable manifold, generate a sequence of gravity assists by selecting good resonances, and target the exit region in the final resonance. This was completed for different values of the Jacobi constant, with Table 1 showing the resulting resonance sequences and ΔV sums for each trajectory.

Table 1: Resulting sequence of resonances for various Jacobi constant with total ΔV required to target Poincarè section taken at periapsis of stable manifold and number of Titan revolutions which is proportional to the total time of flight.

Jacobi Constant	3014	3013	3012	3011	3010	3009
Sequence of Resonances	11:5 - 2:1 - 9:5 - 5:3 - 3:2 - 4:3	11:5 - 2:1 - 9:5 - 5:3 - 3:2 - 4:3	11:5 - 2:1 - 9:5 - 5:3 - 3:2 - 7:5	11:5 - 2:1 - 9:5 - 5:3 - 3:2 - 4:3	11:5 - 2:1 - 9:5 - 8:5 - 4:3	11:5 - 2:1 - 9:5 - 5:3 - 3:2 - 4:3
ΔV	13.70	27.19	15.99	31.73	24.11	37.12
No. Titan Revolutions	34	34	37	34	34	34

Although there is no clear trend in the total number of Titan revolutions, and therefore total time of flight, for varying Jacobi constants, the results shown in Table 1 and graphically represented in (ω, K) space in Figure 5, demonstrate that the choice of Jacobi constant affects some key aspects in the design of the trajectory. Firstly, the Jacobi constant affects the trajectories comprising the stable invariant manifolds – thus, the Poincarè section used to create the exit region changes. Represented as a light blue filled curve in the figure, this region can vary significantly with respect to minimum and maximum semimajor axis and periapsis angles, as demonstrated by the difference between Figure 5a) and Figure 5c).

This change in the exit region affects the set of resonances that intersect with it. In addition to changing the number of available resonances or the minimum n value of these resonances, its position along the ω axis can shift. For a given maximum value of control input, this shifting could cause the target region to be unreachable from a particular resonance at one Jacobi constant, while it is reachable for another Jacobi constant. Such a difference is evident in Figure 5 b) and c) which traverse the same sequence of resonances until the final resonance. Another reason for this difference in resonance sequences can be postulated by looking at Figure 5 a) and b). Looking at the fourth resonance on these two plots, it is evident that the value of the Jacobi constant can affect the range of available resonances. Using the aforementioned method of surveying resonances which can be reached by starting at a periapsis angle of $\omega = (0, 0.15]$, the 5:3 resonance falls within this range for $C_J = 3.012$, while it is not for $C_J = 3.010$. Algorithms performing this calculation would require some form of adaptive decision-making to decide on the merits of extending this interval. In this particular case, the time of flight for the $C_J = 3.010$ trajectory is not larger than that of $C_J = 3.012$ and such a tradeoff may not be too pertinent.

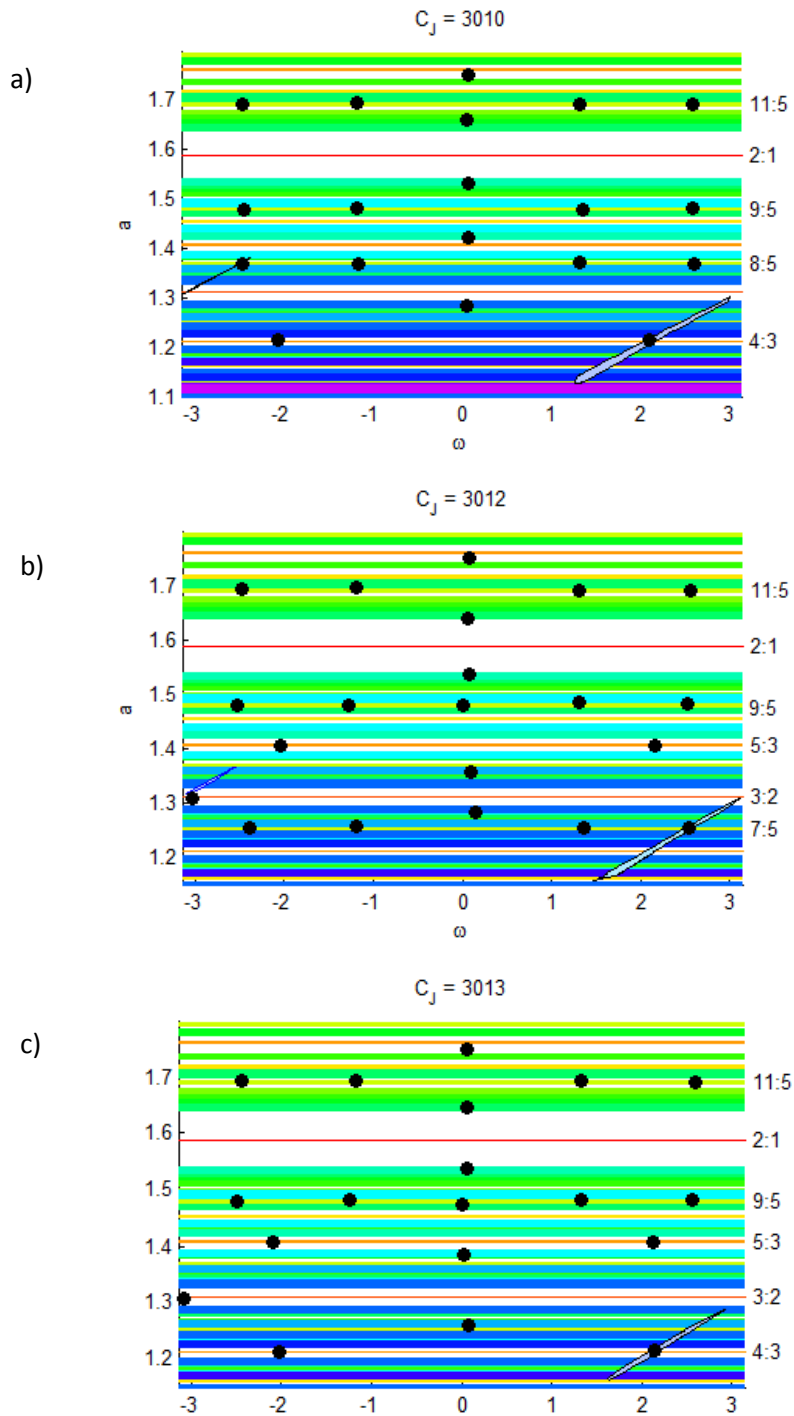


Figure 5: Resonant gravity assist trajectories created using selective resonance targeting plotted for a) $C_j = 3.010$ b) $C_j = 3.012$ and c) $C_j=3.013$. Trajectory (black dots) and target regions (blue filled curves) plotted against resonances with traversed resonances labeled to the right.

4. Methods

4.1. Invariant Manifolds

4.1.1. Planar Circular Restricted Three-Body Problem (PCR3BP)

Construction of the invariant manifolds in the Saturn-Titan system relies on the following problem definition: two main bodies, referred to as primaries, revolve around their barycenter with a test mass, the spacecraft, moving in a planar circular orbit under the influence of the gravitational attraction of the primaries.¹ In the problem of interest, the two primaries, Saturn and Titan, are respectively assigned normalized masses of $m_1 = 1 - \mu$ and $m_2 = \mu$, where $\mu = \frac{M_2}{M_1 + M_2}$. As shown in Figure 6, the primaries are located at $(-\mu, 0)$ and $(1 - \mu, 0)$, respectively, in the Saturn-Titan rotating frame. In the PCR3BP, the motion of the test particle with location (x, y) is governed by the following equations³:

$$\ddot{x} - 2\dot{y} = \frac{\partial \Omega}{\partial x} \quad (1)$$

$$\dot{y} + 2\dot{x} = \frac{\partial \Omega}{\partial y} \quad (2)$$

Where

$$\Omega(x, y) = \frac{x^2 + y^2}{2} + \frac{1 - \mu}{\sqrt{(x + \mu)^2 + y^2}} + \frac{\mu}{\sqrt{(x - 1 + \mu)^2 + y^2}}. \quad (3)$$

The effective potential, Ω , in Eq (3) gives rise to five Lagrange points whereby the gravitational force on the test mass is negated by the centripetal force.⁶ These Lagrange points are marked in Figure 1 as L_i $i=1, 2, 3, 4, 5$. Of most interest in this problem is L_2 , one of the unstable collinear equilibrium points.

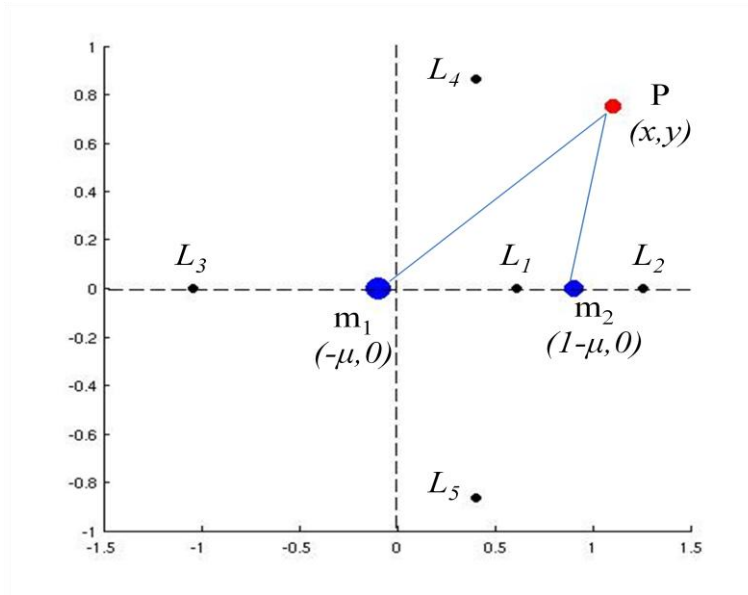


Figure 6 : PCR3BP Geometry and Lagrange Points. In the Saturn-Titan-spacecraft system, m_1 is Saturn, m_2 is Titan, and P is the spacecraft.

Considering the Hamiltonian as a function of positions and velocities, the following energy integral is obtained³:

$$E(x, y, \dot{x}, \dot{y}) = \frac{1}{2}(\dot{x}^2 + \dot{y}^2) - \Omega(x, y) \quad (4)$$

4.1.2. Regions of allowable motion

Fixing the energy integral such that it is equal to a constant allows one to project the corresponding 3D surface onto position space, where (x, y) are coordinates in the Saturn-Titan rotating frame. This projection is referred to as the Hill's region. Bounding this region in position space are zero-velocity curves (i.e. $v = \sqrt{x^2 + y^2} = 0$) which separate regions of allowable and forbidden motion. As seen in Figure 2, the regions accessible to a spacecraft depend on its energy, E , relative to that corresponding to the five equilibrium points. These critical values of energy are defined as³

$$E(L_i) = E(L_i^x, L_i^y, 0, 0) = \Omega(L_i^x, L_i^y) \quad (5)$$

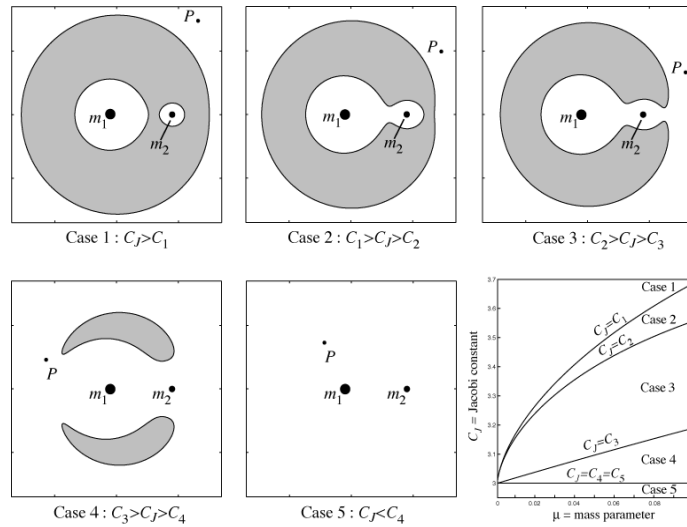


Figure 7: Regions of allowable motion for each energy case; shading indicates forbidden region and white corresponds to allowable motion. Diagram taken from [5].

The shaded regions in Figure 7 correspond to forbidden regions. In the case of $E < E_1$, the shaded annulus separates the exterior and interior regions of allowable motion. For the problem being considered, the spacecraft shall begin at a very large semimajor axis relative to the Saturn-Titan system. At the end of the trajectory, it is intended that the spacecraft will be captured at Titan. These mission requirements mean that the spacecraft should have an energy, E , such that it can move from the exterior region to the interior region of the Saturn-Titan system. This motion is possible in the case of $E(L_2) < E < E(L_3)$.³

4.1.3. Invariant Manifolds

Creation of the invariant manifolds begins with the selection of an initial condition from a Lyapunov orbit about L_2 . This periodic orbit is found by creating a family of periodic orbits about L_2 beginning from a linearized approximation to the Lyapunov orbit. Differential correction is then used to obtain the orbit corresponding to the energy of the spacecraft to within a certain tolerance level. The state transition matrix, $\Phi(T, 0)$, is then calculated over one period. Using the eigenvectors of this matrix, local approximations to the stable and unstable manifolds can be found. This state vector can then be integrated using nonlinear equations of motion to create the stable and unstable manifolds.⁷ The invariant manifolds for a Jacobi constant of 3.012 for a gravitational parameter of $\mu = 2.3663 \cdot 10^{-4}$ are shown in Figure 8. The points highlighted

in green denote the periapsis of those trajectories that form the stable manifold – these points will be targeted by the resonant gravity assist portion of the trajectory.

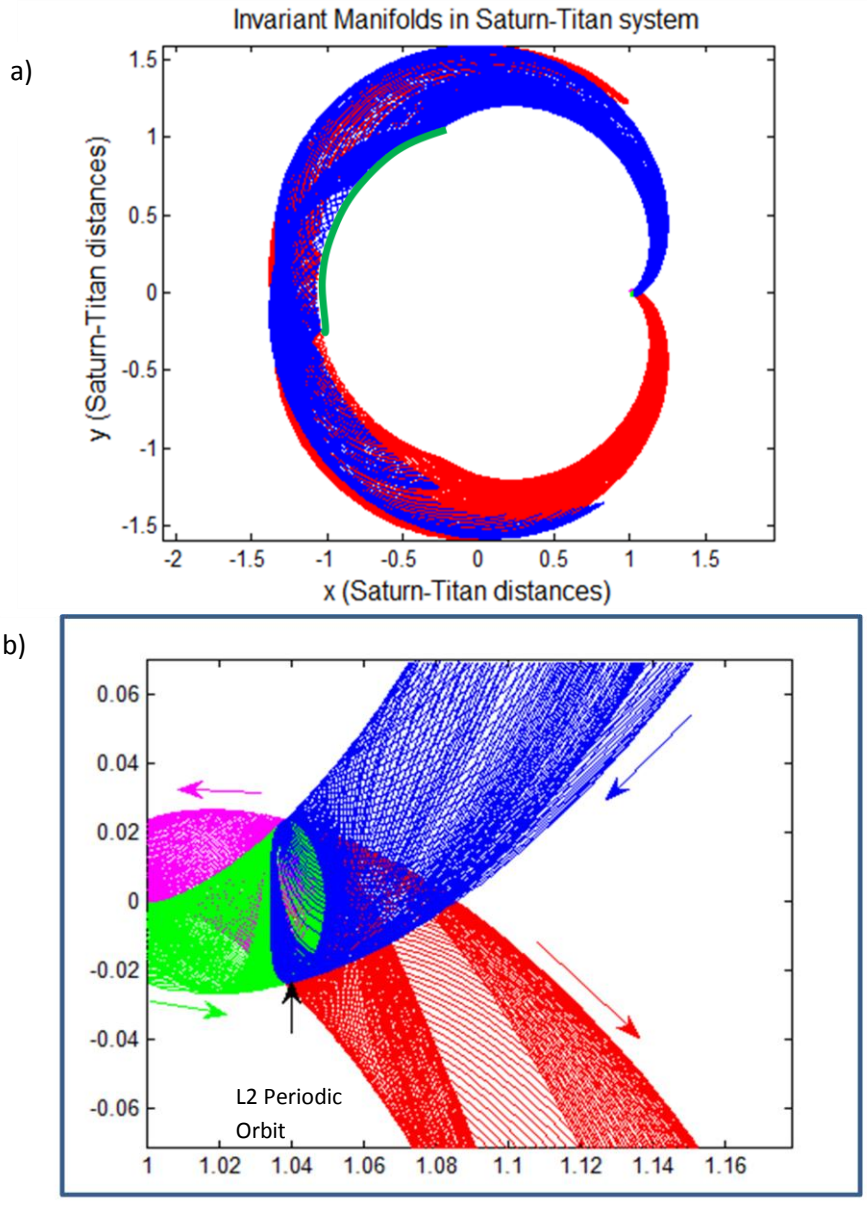


Figure 8 : Invariant manifolds in the Saturn-Titan-spacecraft system. a) The green curve shows the intersection of the stable manifold with the Poincarè section at periapsis. b) Zoomed view of invariant manifolds emanating from L₂ periodic orbit. Red and magenta tubes are unstable manifolds, while green and blue tubes are stable manifolds. Arrows show direction of motion with respect to time.

4.2. Resonant Gravity Assists

4.2.1. Keplerian Map

Since the invariant manifolds in the Saturn-Titan-spacecraft and the Sun-Saturn-spacecraft PCR3BP do not intersect, it is possible to employ resonant gravity assists to reduce the semi-major axis of the spacecraft's orbit about Saturn with minimal fuel usage. Recalling the PCR3BP constructed in Section 4.1, Figure 9 further defines the osculating orbital elements for the spacecraft, the test particle, as it moves with near-Keplerian motion about m_1 and m_2 , and Saturn and Titan, respectively.⁶

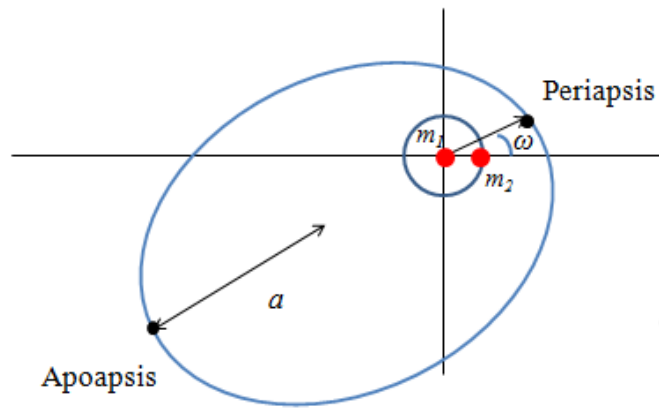


Figure 9 : Osculating orbital elements in the PCR3BP, considering an inertial frame of reference where a is the semi-major axis and ω is the angle of periaapsis.

The spacecraft begins in an orbit of large semimajor axis about Saturn, in the exterior realm. At the periaapsis of the spacecraft's orbit, it receives its largest perturbation. This perturbation can be modeled as an instantaneous event occurring at periaapsis, approximated by an energy kick function⁵:

$$f(w, K) = \frac{\Delta G}{\mu} \quad (6)$$

where

$$\Delta G = -\frac{\mu}{\sqrt{p}} \left[\left(\int_{-\pi}^{\pi} \left(\frac{r}{r_2} \right)^3 \sin(\omega + v - t(v)) dv \right) - \sin\omega \left(2 \int_0^{\pi} \cos(v - t(v)) dv \right) \right] \quad (7)$$

and

$$K = -\frac{-1}{2a} . \quad (8)$$

Here, $\nu = \nu(t)$ is the true anomaly of the particle, $p = \sqrt{a(1 - e^2)}$ is the angular momentum of the spacecraft's orbit, r is the distance between the test particle and the m_1 - m_2 barycenter, and r_2 is the distance between the test particle and m_2 .⁶ An example plot of the energy kick function for $C_J = 3.012$ is shown in Figure 10. Varying the Jacobi constant or average semimajor affects the amplitude of the maximum kick available at periapsis and the periapsis angle, ω , at which this occurs.

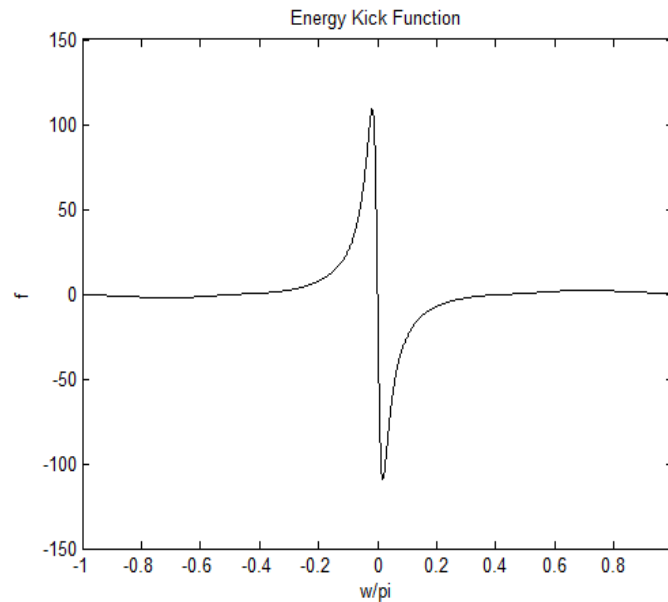


Figure 10 : Energy kick function for $C_J = 3.012$. The minimum of the function, located at $\omega = 0.058$ produces the largest possible decrease in semimajor axis while the maximum of the function at $\omega = -0.058$ produces the largest increase in semimajor axis.

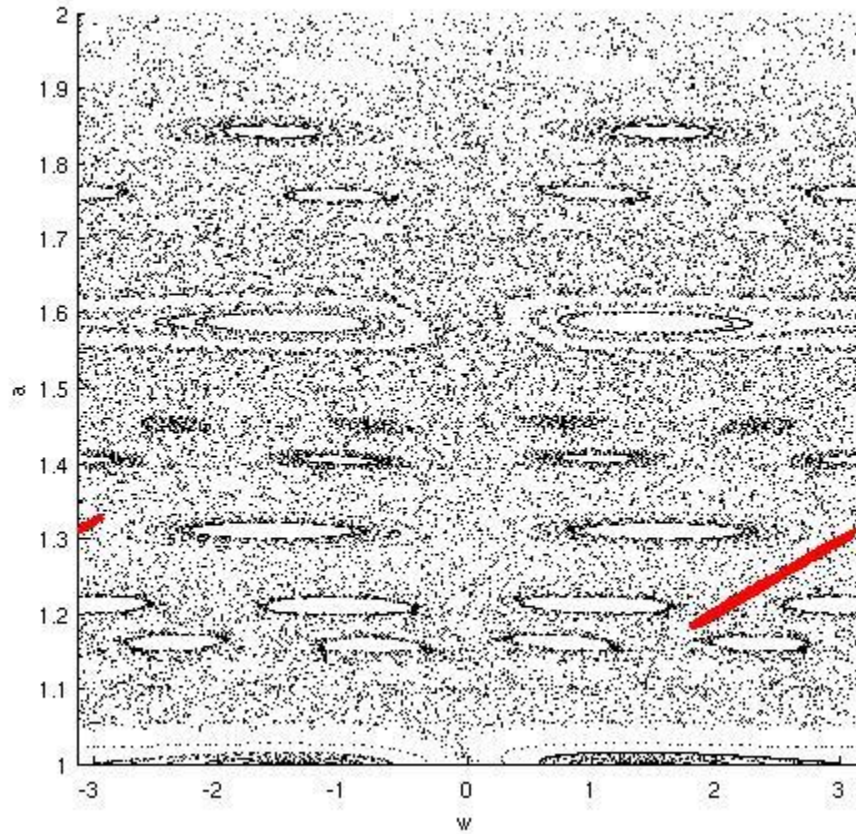


Figure 11 : Keplerian map for the Saturn-Titan system, assuming $C_J = 3.012$ and an average semimajor axis of 1.55. The white holes indicate stable resonant islands, while the red curve represents the target region corresponding to the Poincaré section of the stable manifold at periapsis.

Considering only the effect of the gravitational force on the semi-major axis, and therefore the Keplerian energy, $K = \frac{-1}{2a}$, the following two-dimensional map² can approximate the sequence of periapsis coordinates (ω_n, K_n) , $n=1, 2, 3, \dots$, from an initial (ω_0, K_0) :

$$F \begin{pmatrix} \omega_n \\ K_n \end{pmatrix} = \begin{pmatrix} \omega_{n+1} \\ K_{n+1} \end{pmatrix} = \begin{pmatrix} \omega_n - 2\pi(-2K_{n+1})^{-\frac{3}{2}} \pmod{2\pi} \\ K_n + \mu f(\omega_n) \end{pmatrix} \quad (9)$$

Employing control, however, over each orbit allows for targeting of angles in order to cause a predicted change in semi-major axis. A ΔV is best exerted at apoapsis or periapsis to avoid any out-of-plane motion, changing the Keplerian map as follows²:

$$F \begin{pmatrix} \omega_n \\ K_n \end{pmatrix} = \begin{pmatrix} \omega_{n+1} \\ K_{n+1} \end{pmatrix} = \begin{pmatrix} \omega_n - 2\pi(-2K_{n+1})^{-\frac{3}{2}} \pmod{2\pi} \\ K_n + \mu f(\omega_n) + \alpha u_n \end{pmatrix} \quad (10)$$

$$\text{where } \alpha = \sqrt{\frac{1}{\bar{a}} \left(\frac{1+\bar{e}}{1-\bar{e}} \right)} \text{ with } \bar{e} = \sqrt{1 - \left(\frac{C_J - \bar{a}}{2\bar{a}^{3/2}} \right)^2} \text{ and } \bar{a} = -\frac{1}{2K}. \quad (11)$$

This approximation very closely matches the resonant gravity assist trajectory produced via full integration of the equations of motion for the spacecraft in the PCR3BP.

5. Conclusion

In this paper, we have combined invariant manifolds in the planar circular restricted three body problem and multiple gravity assists to design low ΔV trajectories within the Saturn-Titan system. These trajectories have been designed with single-point decision-making based on characteristics of the available resonances, rather than targeting resonances which result in the largest decrease in semimajor axis. Employing the described method of selecting resonances to target has resulted in a significant decrease in the time of flight over the entire trajectory. Using this method, trajectories have been created over a range of Jacobi constants. Although there was no clear trend in the corresponding time of flight or ΔV usage, the study highlighted the importance of selecting the Jacobi constant based on the available resonances given a series of resonances to be targeted and the maximum ΔV available for maneuvers.

Although the presented method of single-point decision-making has resulted in a large decrease in the total time of flight for a relatively similar value of ΔV over the gravity assist portion of the trajectory, a branch and bound decision-making technique may yield a larger decrease in time of flight. This would be a good avenue for future study as the set encompassing all possible combinations could be analyzed to find an optimum.

In addition, there are some limitations to the results presented in Section 3. In particular, the trajectories created would need to be input into a global optimization algorithm to truly optimize for total ΔV . The results presented in Table 1 should merely be used to demonstrate that the choice of Jacobi constant is not an arbitrary one.

Finally, it would be interesting to include the ΔV at capture when studying the effect of the Jacobi Constant. As the Jacobi constant changes, so too does the radius of the spacecraft before capture – therefore, the capture ΔV will exhibit changes. While this contribution is significantly larger to the minute ΔV 's for the gravity assist and invariant manifold portions of the trajectory, the capture ΔV may add to any possible trends or considerations.

Implementing these steps for future work would surely contribute to current efforts in designing trajectories with low ΔV – allowing us to expand our envelope of feasible and affordable space exploration.

6. Acknowledgements

I would firstly like to thank Professor Jerrold Marsden for mentoring me and providing guidance on the project in terms of both direction and in the context of interplanetary exploration. I truly value the experience of joining his group for the summer. In addition, Ashley Moore deserves many thanks for regularly meeting with me to discuss construction of invariant manifolds, providing guidance on the project and as a sounding board for ideas. I would also like to acknowledge my collaboration with Stefano Campagnola who has helped me to develop the gravity assist portion of this project – many thanks for the in-depth discussions, advice and brainstorming sessions. Evan Gawlik, a previous SURF student, deserves a mention for helping me to understand the work he had previously done on the project. Finally, I would like to thank the SURF office for their financial support and providing me with this amazing opportunity.

7. References

- [1] E S Gawlick, J E Marsden, S Campagnola, A Moore, “Invariant Manifolds, Discrete Mechanics, and Trajectory Design for a Mission to Titan,” 2008, AAS_09-226
- [2] S D Ross, S Jerg, O Junge, “Optimal Capture Trajectories using Multiple Gravity Assists,” *Communications in Nonlinear Science and Numerical Simulations*, 2008, pp 4168-4175.
- [3] W S Koon, M W Lo, J E Marsden, S D Ross, “Dynamical Systems, the Three Body Problem and Space Mission Design”, California Institute of Technology, 2006.
- [4] S Campagnola, R Russell, “The Endgame Problem Part A: V-Infinity Leveraging Technique and the Leveraging Graph”, 19th AIAA/AAS Space Flight Mechanics Meeting, 2009.
- [5] S D Ross, DJ Scheeres, “Multiple Gravity Assists, Capture, and Escape in the Restricted Three-Body Problem,” *Siam J Applied Dynamical Systems*, Vol. 6 No. 3, 2007, pp 576-596.
- [6] V. G Szebehely, *Theory of Orbits: the Restricted Problem of Three Bodies*.
- [7] S D Ross, “Cylindrical Manifolds and Tube Dynamics in the Restricted Three-Body Problem,” PhD Thesis, 2004, California Institute of Technology, Pasadena, CA.